Advances in Materials Research, *Vol. 6, No. 1 (2017) 65-78*
DOI: https://doi.org/10.12989/amr.2017.6.1.065

Design and analysis of low velocity impact on thermoplastic hat section with curvilinear profile

Kumresh K Gaur[*1,2], Mayank Dwivedi[2] and Naresh Bhatnagar[1]

[1]*Department of Mechanical Engineering, Indian Institute of Technology Delhi, Hauz Khas, 110016, New Delhi, India*
[2]*Defence Research and Development Organization (DRDO), DRDO Bhawan, Rajaji Marg, 110011, New Delhi, India*

(Received November 3, 2014, Revised April 26, 2017, Accepted April 27, 2017)

Abstract. A hat section was designed and developed for maximum impact energy absorption and/or transmission under low velocity impact. Towards this, different hat sections, having material properties of thermoplastic, were modeled and investigated numerically using finite element analysis (FEA) in the range of 20-50 J impact energy. In the study it was experienced that the design configuration of hat section with curvilinear profile (HSCP) was excellent in energy attenuation capacity and for even distribution of maximum impact force around and along the hat section under low velocity impact loading. To validate the numerical findings, polypropylene copolymer (Co-PP) HSCP and low density polyethylene (LDPE) HSCP were developed and evaluated experimentally in the said impact energy range. A correlation was established between FEA and experimental test results, thereby, validating a numerical model to predict results for other thermoplastic materials under given range of impact energy. The LDPE HSCP exhibited better performance as compared to Co-PP HSCP in the said range of impact energy. The findings of this study will enable the engineers and technologists to design and develop low velocity impact resistance devices for various applications including devices to protect bone joints.

Keywords: hat section; curvilinear profile; low velocity impact; attenuation; numerical; experimental

1. Introduction

Structures having hat sections are known for absorbing and/or transmitting high energy on impact due to even distribution of stresses. David *et al.* (2005) have studied that the open segment of hat section undergoes premature buckling on impact since open segment tends to spread apart, kink and quickly lose shape upon impact. This point of view considered well in this research and therefore, a hat section was designed with curvilinear profile having an upper curved section at the top and curvilinear peripheral flat sections extending toward outer side of said hat section. The peripheral extension of the hat shaped portion stabilizes it during flexion on impact. This result in increased impact strength and energy absorption during impact, hence, reduced tendency to

∗Corresponding author, E-mail: gaur_87@yahoo.co.in

http://www.techno-press.org/?journal=amr&subpage=7 ISSN: 2234-0912 (Print), 2234-179X (Online)

Table 1 Properties of Co-PP and LDPE

Material	Melt flow index* (g/10 min)	Density at 23℃ (g/cm^3)	Flexural modulus (MPa)	Tensile Strength at Yield (MPa)	Tensile Modulus (MPa)	Tensile Elongation at yield (%)	Vicat Softening Point (℃)
Co-PP	10	0.90	900	20	640	6	142
LDPE	30	0.92	140	10	102	40	84

*at 2.16 kg load & 190℃

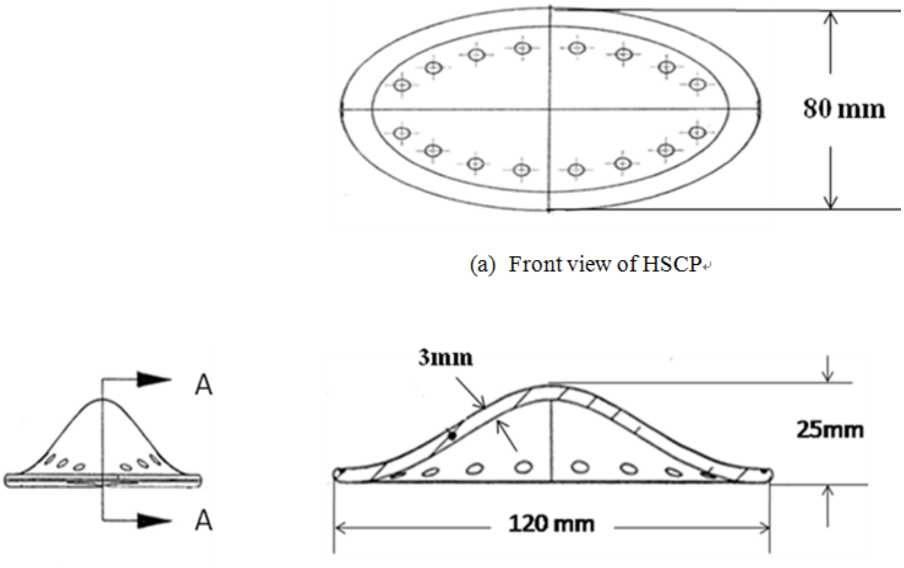

(b)Side elevation view (left side) of HSCP (c) Cross section taken along major axis A-A of HSCP

Fig. 1 Different view of hat section with curvilinear profile (HSCP)

Zakaria *et al.* (2010) have reported the geometry of the component, influences the impact resistance of the component significantly. Gardner *et al.* (2008) have reported that the shapes of most of the bone joints are in the form of ellipsoid with average diameter of 21±5 mm. Yurddaskal *et al.* (2016) have studied the effect of curvature for impact response. HSCPs were designed and developed accordingly. The shape of HSCP was elliptical with major axis and minor axis measuring 120 mm and 80 mm, respectively as shown in Fig. 1(a)-(c). The dimensions of projected hat section were having the height of 25 mm with major and minor axes measuring 70 mm and 30 mm, respectively. HSCPs were made for both the materials. The injection molding conditions were based on the standard ISO 1873-2:2007. Wu *et al.* (2014) have studied the injection moulding parameters such as injection speed, temperature, hold time and rheology to optimize the injection moulding process. The processing conditions for Co-PP; the mold and melt temperature were 45℃ & 240℃ and the maximum holding pressure was 55 MPa. For LDPE, the mold and melt temperature were 35℃ & 215℃ respectively and the maximum holding pressure was 45 MPa. The injection molding machine (Make: Battenfeld HM 40/210 S and Servo electric controlled) having maximum clamping force of 40 kN along with 25 mm diameter general purpose screw was used for molding of HSCPs.

3.3.2 Plastic response of the HSCP under impact

In elastic collisions, energy is lost and none goes into yielding or frictional resistance. In general, the designs which are rugged enough to withstand large collisions elastically are heavy. In elastic idealization, the deformation behaviour is linear-the force needed to deform or deflect the test specimen (HSCP) is proportional to the displacement. In practice the force variation is linear only up to the onset of yielding or crushing, which occurs without further increase in resistance. The limiting load may be taken as the load at the onset of yielding for axially loaded specimen or the load require to produce onset of plastic deformation in test specimen.

Fig. 2 shows idealized elastic plastic behaviour in general. The hashed area represents the energy absorbed by a HSCP undergoing yielding. Ravid and Bodner (1983) have studied the displacement increases linearly up to the limit load, F_u after which the specimen deforms without additional force. The energy integral is simply the area under the curve as given in Eq. (4).

$$E_p = \int_o^y F du = F_u y_{\max} - \frac{F_u^2}{2k} \tag{4}$$

Equating the kinetic energy of impact and the strain energy gives HSCP deformation as given in Eq. (5).

$$y_{\max} = \frac{Ek + \frac{F_u^2}{2k}}{F_u}, \text{ where } k\text{=Amount of weight required to deflect a specimen} \tag{5}$$

The displacement, y_{max}, is limited in practice by the ability of HSCP to absorb plastic deformation without becoming unstable.

The ratio of the total deformation to the elastic deformation is conventionally called the 'ductility factor,' μ. The ductility factor relates elastic capacity of HSCP and impact load in a useful way, using a simple energy balance. Suppose HSCP is subjected to an external load, F, equating the work done by impact force, Fy_{max}, to energy absorbed by HSCP as shown in the Fig. 2 which provides the following energy balance as given in Eq. (6).

$$Ey_{\max} = \frac{1}{2} F_u y_u + F_u (y_{\max} - y_u) or \frac{F_u}{F} = \frac{2\mu}{2\mu - 1}, \text{ Where: } \mu = \text{ the ductility factor, } \frac{Y_{\max}}{y_u} \tag{6}$$

The relationship expresses the required capacity of HSCP for elastic deformation; F_u is the anticipated load to which certain degree of damage is to be tolerated.

As per empirical equation, ductility factor exceeding 10 is associated with very heavy damage whereas; the ductility factor below 5 produces tolerable damage which will probably allow HSCP to be used again.

3.3 Numerical simulation and finite element model implementation

Sezer *et al.* (2007) have reported the FEA is to divide the body into finite elements, often just called elements. It is designed to contain the structural properties and the material which specifies how the structure will react under specific loading conditions. Duan *et al.* (2003), Dean *et al.* (2003), Kharazan *et al.* (2015) and Aghaei *et al.* (2015) have studied that the analysis of multiaxial impact behaviour and finite element method are important for simulation and prediction of deformation of polymers and composites under low velocity impact. Zouambi *et al.* (2014) have modeled the bone joints for computational analysis and predicted the stress behavior. In this study, for numerical analysis, a commercially available finite element analysis code ANSYS Ver.13 (Explicit STR) was used to simulate the falling conditions of a drop weight for different descend

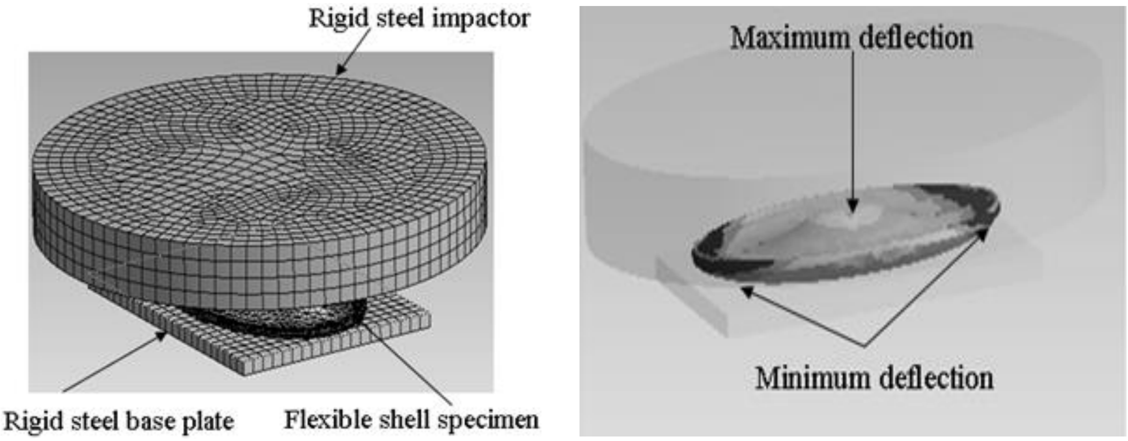

(a) FEA models of HSCP (b) Simulated effective deformation

Fig. 3 FEA models of HSCP

Finally the positions are updated to time n+1 by integrating the velocities through Eq. (14).

$$x_i^{n+1} = x_i^{n} + \dot{x}_i^{n+1/2} + \Delta t^{n+1/2} \tag{14}$$

By using this method for time integration for nonlinear problems, the equations became uncoupled and could be solved directly (explicitly). There was no requirement for iteration during time integration. No convergence checks were needed since the equations were uncoupled and no inversion of the stiffness matrix was required.

Courant *et al.* (1967) have studied to ensure stability and accuracy of the solution, the size of the time step used in explicit time integration is limited by the Courant-Friedrichs-Levy condition. This condition implies that the time step be limited such that a disturbance (stress wave) cannot travel further than the smallest characteristic element dimension in the mesh, in a single time step. Thus the time step criteria for solution stability is given by Eq. (15).

$$\Delta t \leq f * \left[\frac{h}{c}\right]_{\min} \tag{15}$$

Where Δt is the time increment, f is the stability time step factor h is the characteristic dimension of an element and c is the local material sound speed in an element. With reference to above analysis, settings for this study were finalized by keeping maximum number of cycle 1e+7 and end time 7e-5.

For meshing the geometry of HSCP model, different meshing methods available in ANSYS were tried to assess their effect on mesh density and size. The model was solved in explicit dynamics that examines the time step resulting from different mesh methods. Finally, HSCP geometry meshed by hexahedral mesh was swept through the thickness of the model. The model used in this study contains 9859 nodes and 19015 elements.

Michael (2004) reported threshold value of impact force required for bone hip joints injuries due to fall. Based on these two velocities, were preferred i.e., 2.8 ms^{-1} and 4.2 ms^{-1}. These velocities were used to simulate the falling conditions of a drop weight impact on HSCP. The velocity was increased incrementally from 2.8 to 4.2 ms^{-1} to assess the capability of HSCPs to sustained maximum impact force before failure. An impactor of effective mass of 5.6 kg was

Table 2 Results of force vs deflection behavior

Mode of study	Deflection in Co-PP HSCP		Deflection in LDPE HSCP	
	At LVI (2.8ms^{-1}) (impacted energy 21.9 J)	At MVI (4.2ms^{-1}) (impacted energy 49.4 J)	At LVI(2.8 ms^{-1}) (impacted energy 21.9 J)	At MVI (4.2 ms^{-1}) (impacted energy 49.4 J)
Numerical Analysis	12.8 mm	19.1 mm	7.3 mm	12.5 mm
Experimental Analysis	11.0 mm	17.4 mm	6.9.0 mm	11.3 mm

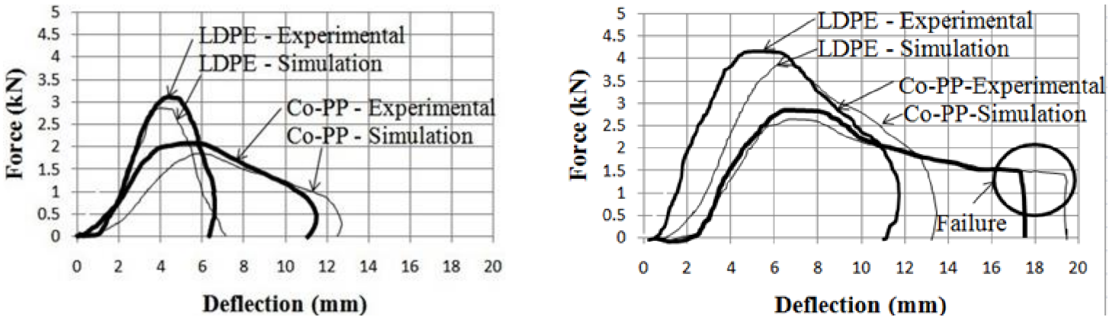

(a) At impact energy 21.9 J (b) At impact energy 49.4 J

Fig. 4 Force vs deflection behavior of Co-PP and LDPE HSCP

Table 3 Results of absorbed energy vs time behavior

Mode of study	Energy absorbed by Co-PP HSCP		Energy absorbed by LDPE HSCP	
	At LVI (2.8ms^{-1}) (impacted energy 21.9 J)	At MVI (4.2ms^{-1}) (impacted energy 49.4 J)	At LVI(2.8 ms^{-1}) (impacted energy 21.9 J)	At MVI (4.2 ms^{-1}) (impacted energy 49.4 J)
Numerical Analysis	11.0 J	22.5 J	12.5 J	29.0 J
Experimental Analysis	12.5 J	25.0 J	14.0 J	31.0 J

sustainability of HSCPs to be used as safety gears to prevent injuries and to assess the limit of HSCPs to sustain impact energy before failure.

4.1 Force vs deflection behavior

The low velocity (2.8 ms^{-1}) and moderate velocity (4.2 ms^{-1}) signify impact energies of 21.9J and 49.4 J, respectively. The results of FEA simulation and experiments for LVI and MVI in cases of LDPE HSCP and Co-PP HSCP are tabulated in Table 2.

The plots of these values for instant comparison at different deflections are given in Fig. 4(a)-(b). It was also evaluated from plots that FEA values are in close comparison with experimental values, thus, validating the numerical findings for force Vs deflection behavior.

From Fig. 4(b), it was also observed that Co-PP HSCP, at 49.4 J impact energy elongated and stretched along the deformation axis with small reduction in impact force and finally exhibited an unexpected sudden drop in impact force. This was attributed to the catastrophic damage and eventually a fracture of the Co-PP HSCP. Whereas, no failure behaviour was observed for LDPE HSCP either in experiments or in FE based numerical analysis at impact energy of 49.4 J. This was

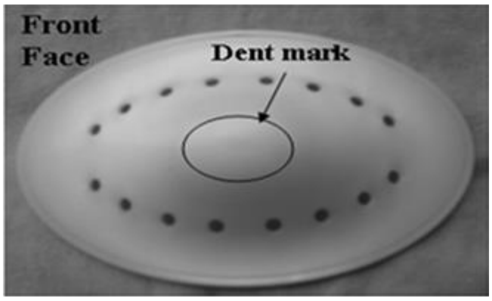

(a) Front surface of Co-PP HSCP at impact energy 21.9 J

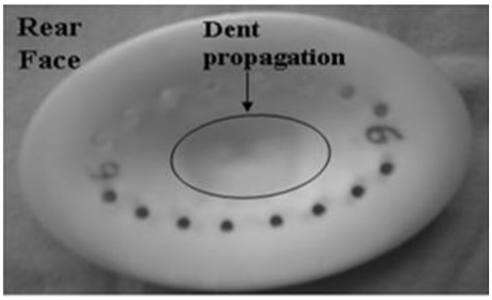

(b) Bottom surface of Co-PP HSCP at impact energy 21.9 J

(c) Front surface of LDPE HSCP at impact energy 21.9 J

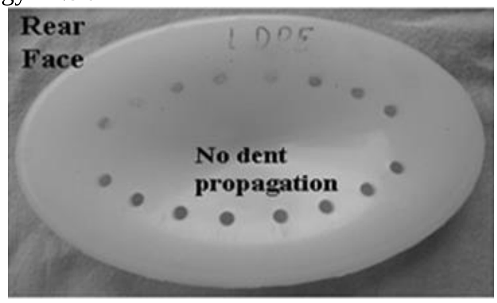

(d) Bottom surface of LDPE HSCP at impact energy 21.9 J

Fig. 7 Impact damage behavior of Co-PP and LDPE HSCP

resulting in higher impact energy absorption and superior spring back property of the LDPE HSCP compared to Co-PP HSCP.

4.3 Force vs time behavior

The force vs time behavior results of FEA simulation and experiments for LVI and MVI in the cases of LDPE HSCP and PP HSCP are tabulated in Table 4.

Force vs time graphs are shown in Figs. 6(a)-(b) illustrated that the impact force increases with increase in impact energy. From the curves it is observed that LDPE HSCP has higher force carrying capacity compare to Co-PP HSCP at both the impacted energies. FEA results are in close comparison with the experimental results for all impact energies. Thus testifying the validating of numerical model for force vs time behavior.

From above results, it is observed that the small variation existed between numerical and experimental results. The reason for this might be attributed to the limitations of numerical model used in this study. The model exercised in this study was based on a number of assumptions and simplifications. The validity and correctness of these models depend on mechanical loading, geometry of the part, material characteristics, mechanical properties during experiments and data used in FEA simulations. There is an always a gap in values of theoretically exerted load and actually experienced load by test specimen. Similar, the multiaxial distribution and resulting stresses, occur in actual experiment, are difficult to simulate in FEA simulation. However, in this study, due to axis symmetric body in the form of HSCP produces close compromise in the value of FEA simulation and experimental data. Further, this model also has not taken into account the

A higher impact damage resistance of the LDPE HSCP, compared to Co-PP HSCP, was observed due its better interfacial adhesion among polymeric chains and semicrystalline nature. Furthermore, long molecular chain and high molecular weight of LDPE significantly enhanced the absorption of impact energy compared to Co-PP which has shorter molecular chains and lower molecular weight.

5. Conclusions

In this study, the numerical model of a curvilinear hat profile made out of two different thermoplastics (CoPP and LDPE) was validated experimentally for a low velocity impact. This numerical model facilitated a close prediction of energy absorption behaviour of both the thermoplastics under low velocity impact up to 49.4 J. The study also revealed that the low velocity damage resistance of curvilinear hat profile of LDPE is found to be superior to CoPP. This numerical model indicates its suitability for design and analysis of range of thermoplastic products such as automotive parts, sports/recreational goods, medical devices etc., which experience low velocity impacts.

References

Aghaei, M., Forouzan, M.R., Nikforouz, M. and Shahabi, E. (2015), "A study on different failure criteria to predict damage in glass/polyester composite beams under low velocity impact", *Steel Compos. Struct.*, **5**(18), 1291-1303.

Balasubramani,V., Rajinder B.S. and Vasudevan, R. (2013), "Numerical analysis of low velocity impact on laminated composite plates", *Proc. Eng.*, **64**, 1089-1098.

Courant, R., Friedrichs, K. and Lewy, H. (1967), "The partial difference equations of mathematical physics", *IBM*, 215-234.

Daiyan, H., Andreassen, E., Grytten, F., Lyngstad, O.V., Luksepp, T. and Osnes, H. (2010), "Low-velocity impact response of injection-moulded polypropylene plates-part 1: Effects of plate thickness, impact velocity and temperature", *Polym. Test*, **29**(6), 648-657.

Dean, G. and Wright, L. (2003), "An evaluation of the use of finite element analysis for predicting the deformation of plastics under impact loading", *Polym. Test.*, **22**(6), 625-631.

Drozdov, A.D., Al-Mulla, A. and Gupta, R.K. (2012), "Structure-property relations for polymer melts: Comparison of linear low-density polyethylene and isotactic polypropylene", *Adv. Mater. Res.*, **4**(1), 245-268.

Duan, Y., Saigal, A., Greif, R. and Zimmerman, M.A. (2002), "Analysis of multiaxial impact behavior of polymers", *Poly. Eng. Sci.*, **42**(2), 395-402.

Flores-Johnson, E.A. and Li, Q.M. (2011), "Low velocity impact on polymeric foams", *J. Cell. Plast.*, **47**(1), 45-63.

Gardner, M.J., Robertson, W.J., Boraiah, S., Barker, J.U. and Lorich, D.G. (2008), "Anatomy of the greater trochanteric 'bald spot: A potential portal for abductor sparing femoral nailing", *Clin. Ortho. Relat. Res.*, **466**(9), 2196-2396.

Heatherington, D., Glasgow, S. and Bruce Lyons, B. (2005), *Vehicle Bumper Beam*, US 20050285416 A1.

Kaur, I., Gupta, N. and Kumari, V. (2013), "Functionalization of polyethylene by graft copolymerization for separation processes", *Adv. Mater. Res.*, **1**(2), 15-36.

Kharazan, M., Sadr, M.H. and Kiani, M. (2014), "Delamination growth analysis in composite laminates subjected to low velocity impact", *Steel Compos. Struct.*, **4**(17), 387-403.

Caihong, L.C., Wu, S., Xu, R., Xu, Y. and Peng, X. (2013), "A study of plastic plateau disappearance in stress-strain curve of annealed polypropylene films during stretching", *Adv. Mater. Res.*, **2**(2), 111-118.

Liu, B., Villavicencio, R. and Guedes, S. (2013), "Experimental and numerical plastic response and failure of pre-notched transversely impacted beams", *Mech. Sci.*, **77**, 314-332.

Ma, Q., Su, X., Lin, Z., Lasecki, J. and Lai, X. (2010), "A constitutive model for the nonlinear viscoplastic behavior of thermoplastic olefin", *Polym. Compos.*, **31**(4), 587-595.

Michael, M. (2004), *Hip Protector System*, US20040049827 A1.

Okayasu, M., Yano, K. and Shiraishi, T. (2014), "Effects of loading conditions on the fatigue failure characteristics in a polycarbonate", *Adv. Mater. Res.*, **3**(3), 163-174.

Plummer, C.J.G. (2004), "Micro deformation and fracture in bulk polyolefins", *Adv. Poly. Sci.*, **169**, 75-120.

Polanco-Loria, M., Clausen, A.H., Berstad, T. and Hopperstad, O.S. (2010), "Constitutive model for thermoplastics with structural applications", *J. Imp. Eng.*, **37**(12), 1207-1219.

Ramakrishnan, K.R. and Shankar, K. (2013), "Experimental and numerical analysis of low velocity impact on plastic laminates", *J. FFEMS*, **36**(11), 1153-1163.

Ravid, M. and Bodner, S.R. (1983), "Dynamics perforation of viscoplastic plates by rigid projectiles", *Eng. Sci.*, **21**(6), 577-590.

Safri, S.N.A., Sultan, M.T.H., Yidris, N. and Mustapha, F. (2014), "Low velocity and high velocity impact test on composite materials-a review", *J. IJES*, **3**, 50-60.

Sezer, H. and Atamturktur, M.S. (2007), "Thesis defence structural assessment of guastavino domes", 10-12.

Spierings, A.B. and Derler, S. (2006), "Assessment of hip protectors and corresponding hip fracture risk using stress calculation in the femoral neck", *Med. Eng. Phys.*, **28**(6), 550-559.

Wright, P.E. (2012), *Introduction to Structural Impact*, PHD Course S164, Meadow Estates Drive, Fairfax, U.S.A.

Wu, C.L. and Lin, C.C. (2014), "Study molded part quality of plastic injection process by melt viscosity evaluation", *Adv. Mater. Res.*, **2**(3), 327-339.

Yurddaskal, M. and Baba, B.O. (2016), "The effect of curvature on the impact response of foam-based sandwich composite panels", *Steel Compos. Struct.*, **5**(20), 983-997.

Zakaria, M., Keith, W., Kambiz, K. and James, N. (2010), "Low velocity impact behavior of glass filled fiber-reinforced thermoplastic engine components", *Mater. Art.*, **3**(4), 2463-2473.

Zouambi, L., Serier, B. and Benamara, N. (2014), "Effect of cavity-defects interaction on the mechanical behaviour of the bone cement", *Adv. Mater. Res.*, **1**(3), 35-45.

CC